

## Globular Cluster Systems of Massive Compact Elliptical Galaxies in the Local Universe: Evidence for Relic Red Nuggets?

JISU KANG<sup>1</sup> AND MYUNG GYOON LEE<sup>1</sup>

<sup>1</sup>*Astronomy Program, Department of Physics and Astronomy, Seoul National University, 1 Gwanak-ro, Gwanak-gu, Seoul 08826, Republic of Korea*

(Received November 27, 2020; Accepted March 30, 2021)

Submitted to ApJ

### ABSTRACT

Nearby massive compact elliptical galaxies (MCEGs) are strong candidates for relic galaxies (i.e. local analogs of red nuggets at high redshifts). It is expected that the globular cluster (GC) systems of relic galaxies are dominated by red (metal-rich) GCs. NGC 1277 is known as a unique example of such a galaxy in the previous study. In this study, we search for GCs in 12 nearby MCEGs at distances of  $\lesssim 100$  Mpc from the Hubble Space Telescope/Wide Field Camera 3 F814W( $I_{814}$ )/F160W( $H_{160}$ ) archival images. We find that most of these MCEGs host a rich population of GCs with a color range of  $0.0 < (I_{814} - H_{160})_0 < 1.1$ . The fractions of their red GCs range from  $f_{RGC} = 0.2$  to  $0.7$  with a mean of  $f_{RGC} = 0.48 \pm 0.14$ . We divide the MCEG sample into two groups: one in clusters and the other in groups/fields. The mean red GC fraction of the cluster MCEGs is  $0.60 \pm 0.06$ , which is  $0.2$  larger than the value of the group/field MCEGs,  $0.40 \pm 0.10$ . The value for the cluster MCEGs is  $\sim 0.3$  larger than the mean value of giant early-type galaxies with similar stellar mass in the Virgo cluster ( $f_{RGC} = 0.33 \pm 0.13$ ). Our results show that most of the MCEGs in our sample are indeed relic galaxies. This further implies that a majority of the red GCs in MCEGs are formed early in massive galaxies and that most MCEGs in the local universe have rarely undergone mergers after they became red nuggets about 10 Gyr ago.

*Keywords:* Compact galaxies (285), Elliptical galaxies (456), Galaxy evolution (594), Globular star clusters (656)

# Globular Cluster Systems of Relic Galaxies

Karla A. Alamo-Martínez,<sup>1,2\*</sup> Ana L. Chies-Santos,<sup>1</sup> Michael A. Beasley,<sup>3</sup>

Rodrigo Flores-Freitas,<sup>1</sup> Cristina Furlanetto,<sup>4</sup> Marina Trevisan,<sup>1</sup>

Allan Schnorr-Müller,<sup>1</sup> Ryan Leaman,<sup>5</sup> Charles J. Bonatto<sup>1</sup>

<sup>1</sup>*Departamento de Astronomia, Instituto de Física, Universidade Federal do Rio Grande do Sul (UFRGS), Porto Alegre, R.S, Brazil*

<sup>2</sup>*Departamento de Astronomía, Universidad de Guanajuato, Apartado Postal 144, 36000, Guanajuato, Guanajuato, Mexico*

<sup>3</sup>*Instituto de Astrofísica de Canarias, Calle Vía Láctea, La Laguna, Spain*

<sup>4</sup>*Departamento de Física, Instituto de Física, Universidade Federal do Rio Grande do Sul (UFRGS), Porto Alegre, R.S, Brazil*

<sup>5</sup>*Max-Planck Institut für Astronomie, Königstuhl 17, D-69117 Heidelberg, Germany*

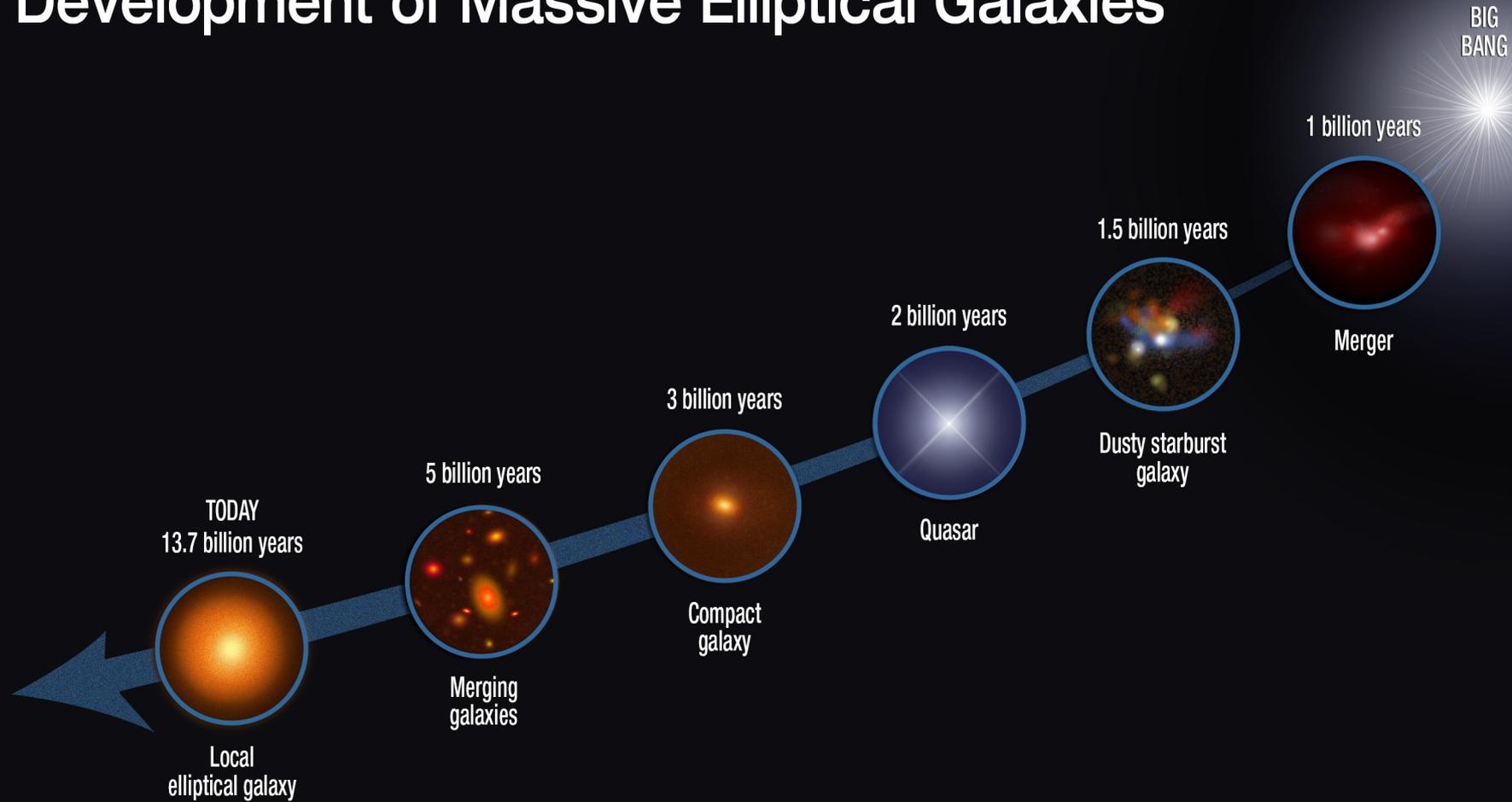
Accepted 2021 February 18. Received 2021 February 17; in original form 2020 December 8

## ABSTRACT

We analyse the globular cluster (GC) systems of a sample of 15 massive, compact early-type galaxies (ETGs), 13 of which have already been identified as good relic galaxy candidates on the basis of their compact morphologies, old stellar populations and stellar kinematics. These relic galaxy candidates are likely the nearby counterparts of high redshift *red nugget* galaxies. Using F814W ( $\approx I$ ) and F160W ( $\approx H$ ) data from the WFC3 camera onboard the *Hubble Space Telescope* we determine the total number, luminosity function, specific frequency, colour and spatial distribution of the GC systems. We find lower specific frequencies ( $S_N < 2.5$  with a median of  $S_N = 1$ ) than ETGs of comparable mass. This is consistent with a scenario of rapid, early dissipative formation, with relatively low levels of accretion of low-mass, high- $S_N$  satellites. The GC half-number radii are compact, but follow the relations found in normal ETGs. We identify an anticorrelation between the specific angular momentum ( $\lambda_R$ ) of the host galaxy and the (I-H) colour distribution width of their GC systems. Assuming that  $\lambda_R$  provides a measure of the degree of dissipation in massive ETGs, we suggest that the (I-H) colour distribution width can be used as a proxy for the degree of complexity of the accretion histories in these systems.

**Key words:** galaxies: star clusters: general – galaxies: evolution – galaxies: formation

# Development of Massive Elliptical Galaxies



# Как образуются red nuggets?

- (1) started with accretion-driven violent disc instability
- (2) contracted via dissipative process, forming compact, star-forming blue nuggets
- (3) star formation in the blue nuggets quenched by feedback due to AGN activity

The blue nuggets became red nuggets about 10 Gyr ago



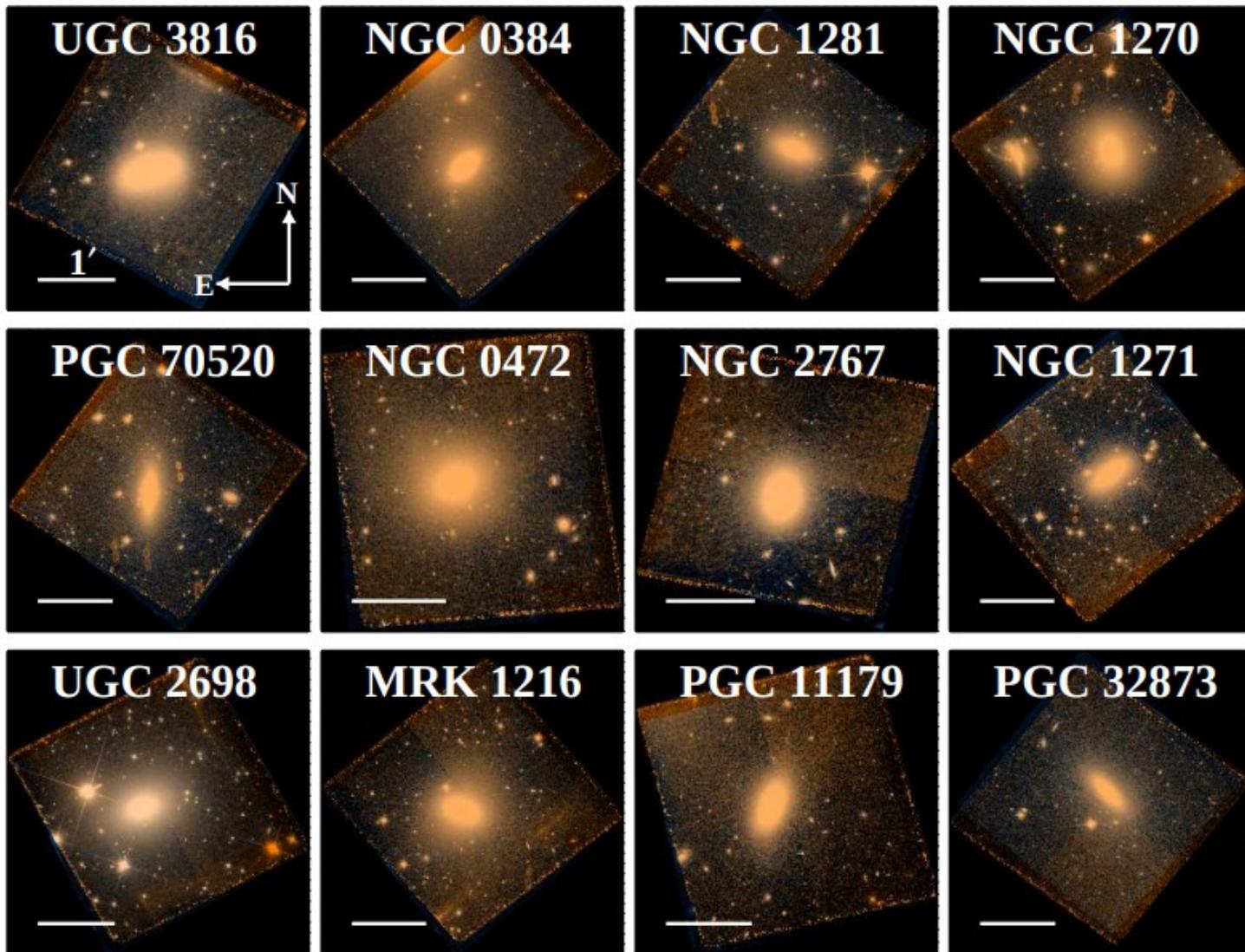
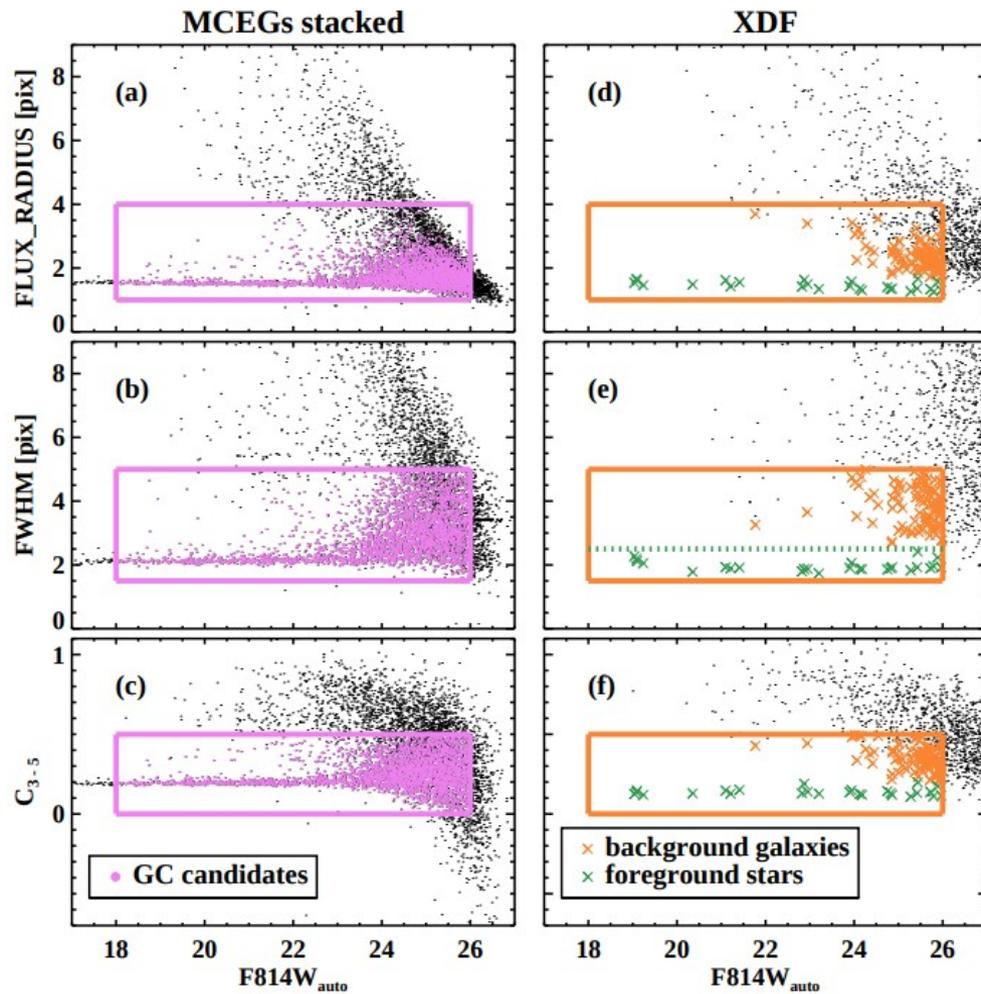


**Table 1.** Basic Properties of the Target MCEGs and Reference Galaxies

Galaxy	$D$ [Mpc]	$R_{e,circ}$ [kpc]	$b/a$	$\sigma_c$ [km s $^{-1}$ ]	$\log(M_*/M_\odot)$	$B$ [mag]	$A_I$ and $A_H$	$f_{RGC}$
(1)	(2)	(3)	(4)	(5)	(6)	(7)	(8)	(9)
UGC 3816	$51 \pm 1$	$1.8 \pm 0.1$	0.69	$251 \pm 7$	$10.96^{+0.06}_{-0.04}$	13.46	0.095, 0.032	$0.51^{+0.12}_{-0.10}$
NGC 0384	$59 \pm 1$	$1.5 \pm 0.1$	0.68	$240 \pm 5$	$10.96^{+0.05}_{-0.05}$	13.67	0.096, 0.032	$0.45^{+0.08}_{-0.09}$
NGC 1281	$60 \pm 1$	$1.3 \pm 0.1$	0.64	$263 \pm 6$	$11.00^{+0.08}_{-0.08}$	13.74	0.256, 0.085	$0.70^{+0.09}_{-0.09}$
NGC 1270	$69 \pm 1$	$1.9 \pm 0.1$	0.68	$376 \pm 9$	$11.31^{+0.10}_{-0.12}$	13.43	0.253, 0.084	$0.61^{+0.06}_{-0.02}$
PGC 70520	$72 \pm 1$	$1.2 \pm 0.1$	0.49	$259 \pm 8$	$10.95^{+0.10}_{-0.12}$	14.17	0.147, 0.049	$0.30^{+0.07}_{-0.07}$
NGC 0472	$74 \pm 1$	$2.0 \pm 0.1$	0.72	$252 \pm 7$	$11.07^{+0.06}_{-0.11}$	13.73	0.075, 0.025	$0.41^{+0.12}_{-0.07}$
NGC 2767	$74 \pm 1$	$1.9 \pm 0.1$	0.75	$247 \pm 9$	$11.12^{+0.09}_{-0.08}$	14.36	0.029, 0.010	$0.37^{+0.01}_{-0.05}$
NGC 1271	$80 \pm 2$	$1.4 \pm 0.1$	0.43	$302 \pm 8$	$11.06^{+0.07}_{-0.07}$	14.30	0.254, 0.085	$0.60^{+0.05}_{-0.05}$
UGC 2698	$89 \pm 2$	$3.1 \pm 0.1$	0.73	$351 \pm 8$	$11.58^{+0.01}_{-0.03}$	13.61	0.224, 0.075	$0.56^{+0.04}_{-0.04}$
MRK 1216	$94 \pm 2$	$2.3 \pm 0.1$	0.58	$335 \pm 6$	$11.34^{+0.11}_{-0.10}$	14.44	0.050, 0.017	$0.52^{+0.09}_{-0.04}$
PGC 11179	$94 \pm 2$	$1.8 \pm 0.1$	0.66	$292 \pm 7$	$11.16^{+0.06}_{-0.08}$	14.51	0.287, 0.096	$0.56^{+0.03}_{-0.11}$
PGC 32873	$112 \pm 2$	$1.9 \pm 0.1$	0.53	$308 \pm 9$	$11.28^{+0.04}_{-0.04}$	14.98	0.019, 0.006	$0.24^{+0.06}_{-0.00}$
NGC 1399	20	11.1	0.91	$332 \pm 5$	11.41	10.60	0.019, 0.006	$0.72^{+0.06}_{-0.10}$
NGC 4874	100	22.7	0.87	$272 \pm 4$	11.76	12.63	0.014, 0.005	$0.55^{+0.08}_{-0.08}$

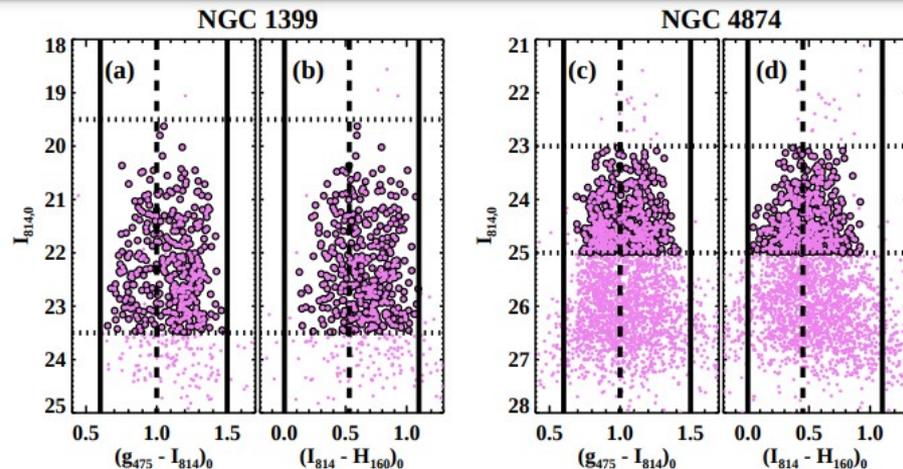
NOTE—(1) Galaxy name; (2) Distances; (3) Effective radii within circularized aperture; (4) The ratio of minor axis and major axis; (5) Central velocity dispersion; (6) Stellar mass derived from simple stellar population models for Salpeter-like stellar IMF (with a slope of  $\Gamma = 2.35$ ); (7) B-band magnitudes; (8) Foreground extinction for F814W( $I_{814}$ ) and F160W( $H_{160}$ ) bands; (9) Fractions of red GCs derived in this study ( $R < 10R_{e,circ}$  for the target MCEGs,  $R \lesssim 1R_e$  for NGC 1399 and  $R \lesssim 2R_e$  for NGC 4874)



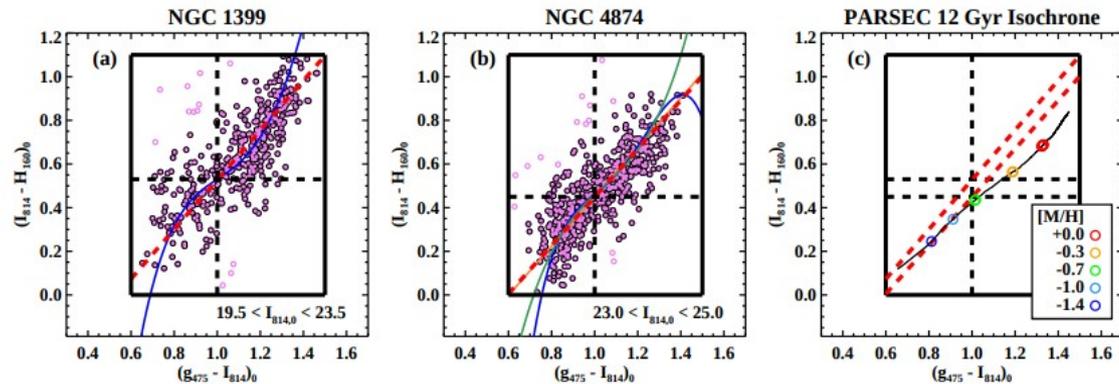
$$C_{3-5} = F814W(r = 3\text{pix}) - F814W(r = 5\text{pix})$$

XDF – Hubble eXtreme Deep Field images

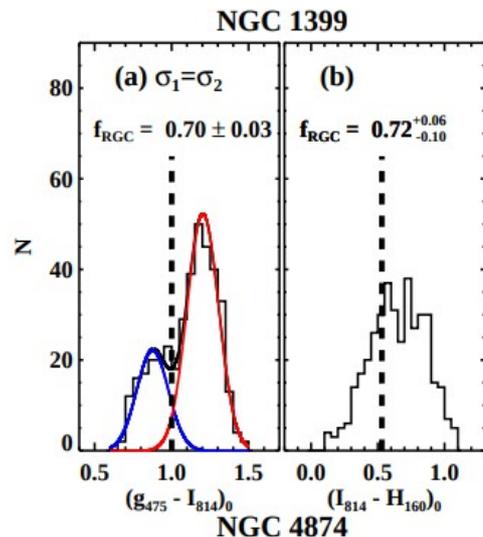
**Figure 2.** (Left panels) Effective radius ( $FLUX\_RADIUS$ ), FWHM, and concentration parameter ( $C_{3-5}$ ) versus  $F814W_{\text{auto}}$  magnitude of the sources detected in the images of the target MCEGs. We plot this diagram after stacking all the results from each MCEG. We mark the selection criteria for GC candidate in pink boxes and selected GC candidates in pink dots. We select the candidates satisfying all three size-related conditions at the same time. (Right panels) Same plots as left panels but for the sources detected in XDF images. We apply the same selection criteria as shown in orange boxes in order to calculate the background contamination. Orange crosses denote background sources and green crosses denote foreground stars with  $FWHM < 2.5$ .



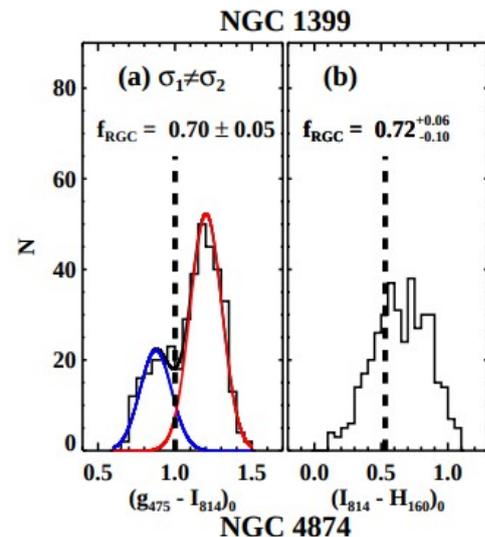
**Figure 4.** CMDs of the GC candidates in (a,b) NGC 1399 and (c,d) NGC 4874. All the GC candidates marked in Figure 3 are also marked in pink dots. The bright GC candidates in NGC 1399 ( $19.5 < I_{814,0} < 23.5$ ) and NGC 4874 ( $23.0 < I_{814,0} < 25.0$ ) are marked in black circles, and the corresponding magnitude ranges are marked in dotted lines. The solid lines denote the color range for selecting the GCs and the dashed lines denote the color used for dividing blue and red GC population.



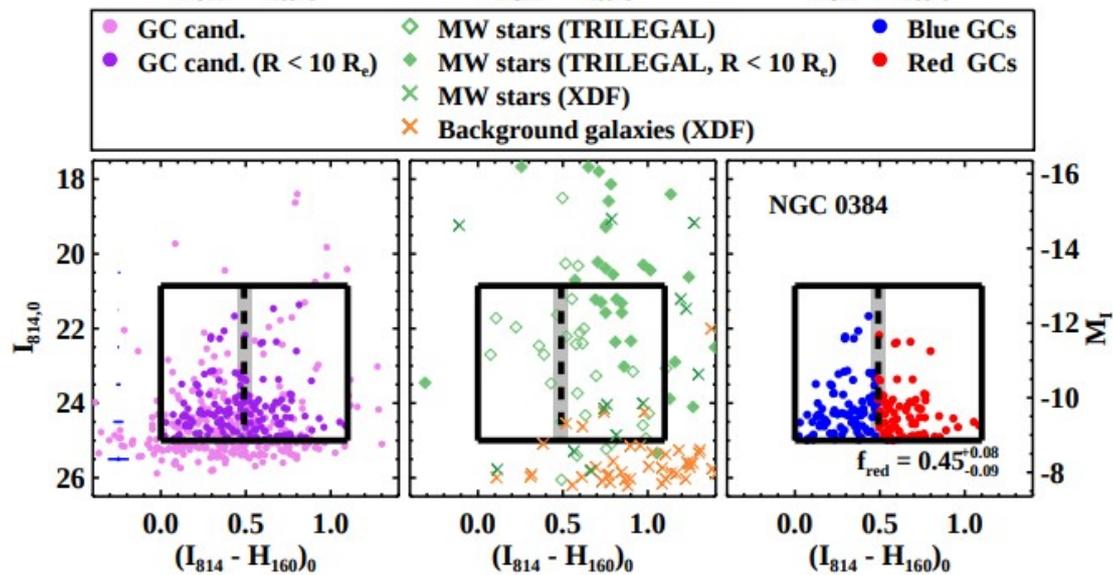
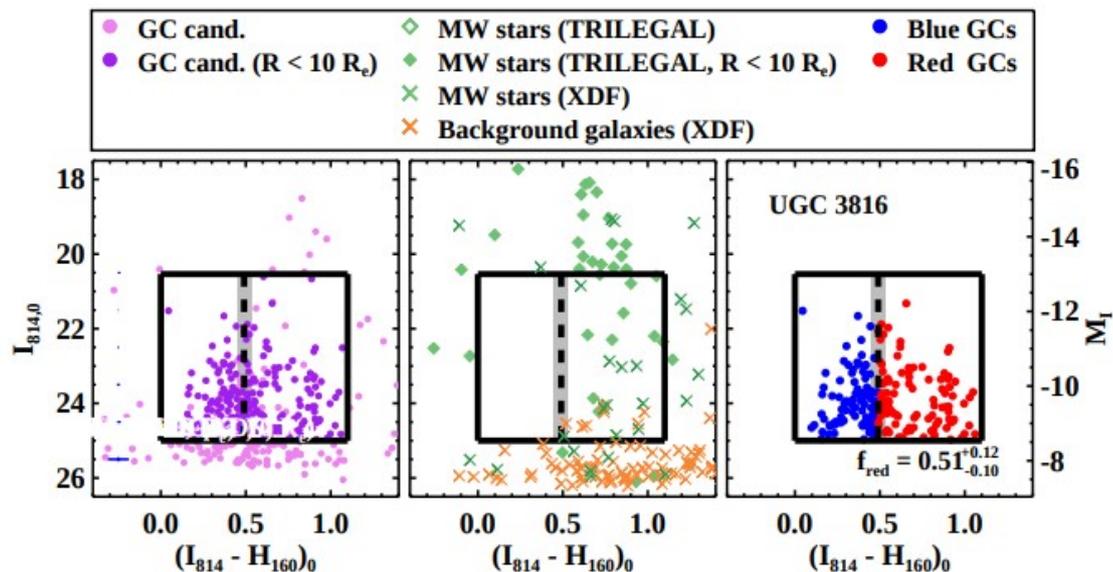
**Figure 5.** Color-color diagrams of the bright GC candidates in (a) NGC 1399 and (b) NGC 4874. The blue line in (a) is a quartic relation for NGC 1399 GCs given by Blakeslee et al. (2012) shifted by  $-0.04$  in y-axis. The orange, green, and blue lines in (b) are linear, cubic, and quartic relations for NGC 4874 GCs given by Cho et al. (2016). The red dashed lines in (a,b) are linear relations derived in this study for each galaxy after  $3\sigma$  clipping. The clipped sources are marked in open pink circles, and filled pink circles are sources used to derive the relation. (c) Color-color relation derived from PARSEC 12 Gyr isochrone. We mark  $[M/H]$  values along with the relation. The same red dashed lines in (a,b) are also marked for comparison. In all the three diagrams, the black solid lines denote the color range for selecting the GCs and the dashed lines denote the color used for dividing blue and red GC populations.

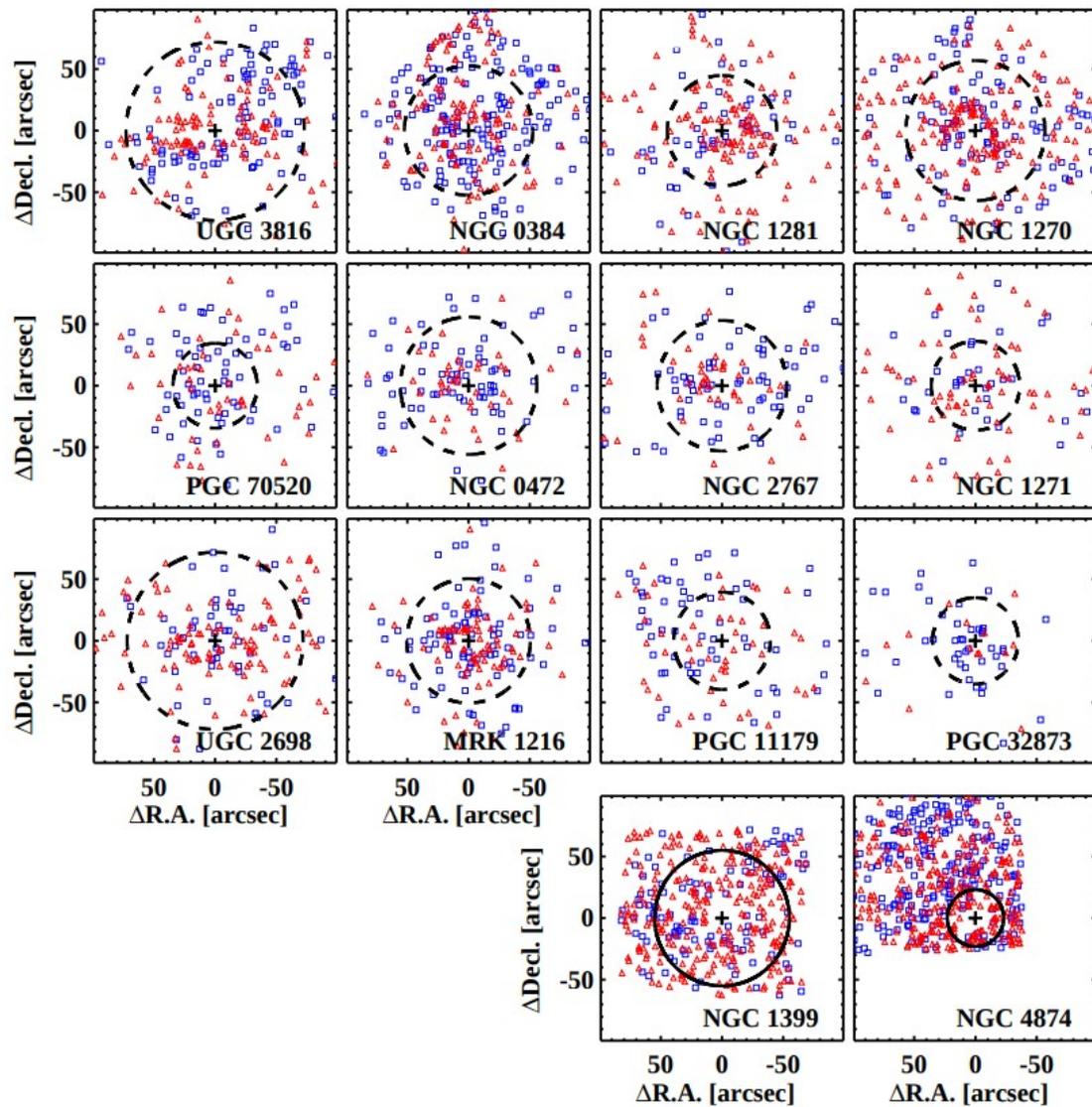


**Figure 6.** Color distributions of the bright GCs in (a,b) NGC 1399 ( $19.5 < I_{814,0} < 23.5$ ) and (c,d) NGC 4874 ( $23.0 < I_{814,0} < 25.0$ ). GMM analysis results for  $(g_{475} - I_{814})_0$  colors with an equal width option are marked in blue and red curves. The dashed lines denote the color used for dividing blue and red GC populations.



**Figure 7.** Same plot as Figure 6 but the GMM analysis results with an unequal width option are marked.





галактики из  
 этой работы

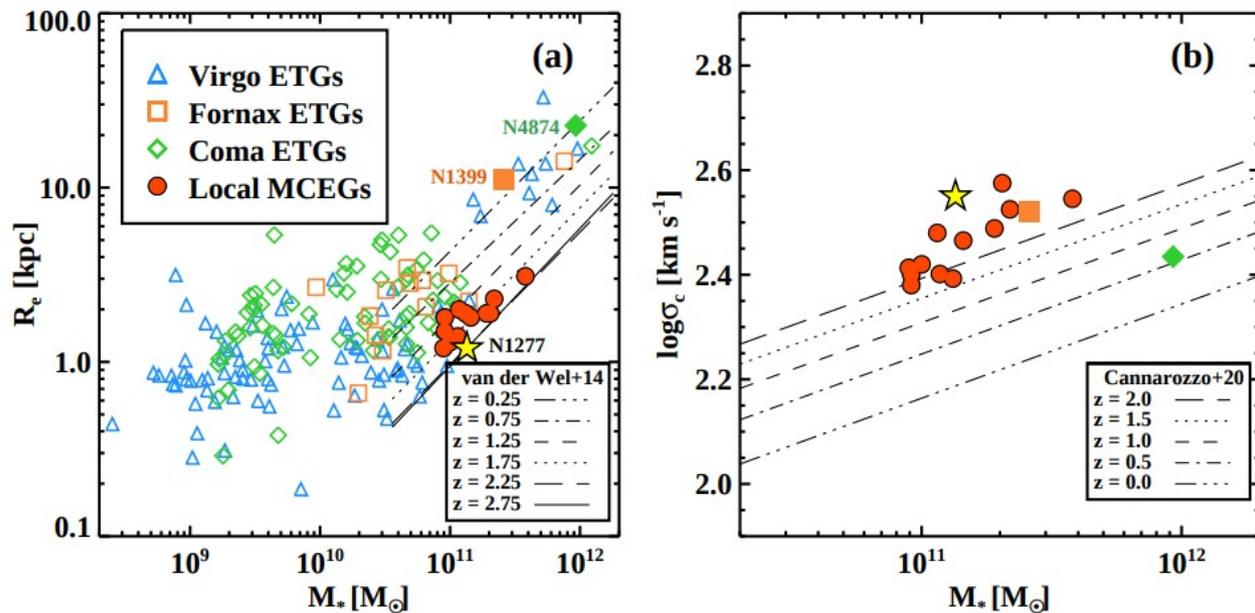


**Figure 16.** (a) Effective radii ( $R_e$ ) vs. stellar masses ( $M_*$ ) for the target MCEGs in this study (filled red circles) in comparison with the Virgo ETGs (blue triangles, Ferrarese et al. 2006; Peng et al. 2008, ACSVCS), the Fornax ETGs (orange squares, Liu et al. 2019, ACSFCS), and the Coma ETGs (green diamonds, Weinzirl et al. 2014, ACSCCS). Filled orange square and filled green diamond denote NGC 1399 and NGC 4874. The yellow star denotes NGC 1277 (Beasley et al. 2018). Black lines are mass-size relations of ETGs at different redshifts (van der Wel et al. 2014). (b) velocity dispersions ( $\log \sigma_c$ ) vs. stellar masses ( $M_*$ ) for the target MCEGs, NGC 1277, and the two reference galaxies. Black lines are mass-velocity dispersion relations of ETGs at different redshifts (Cannarozzo et al. 2020).

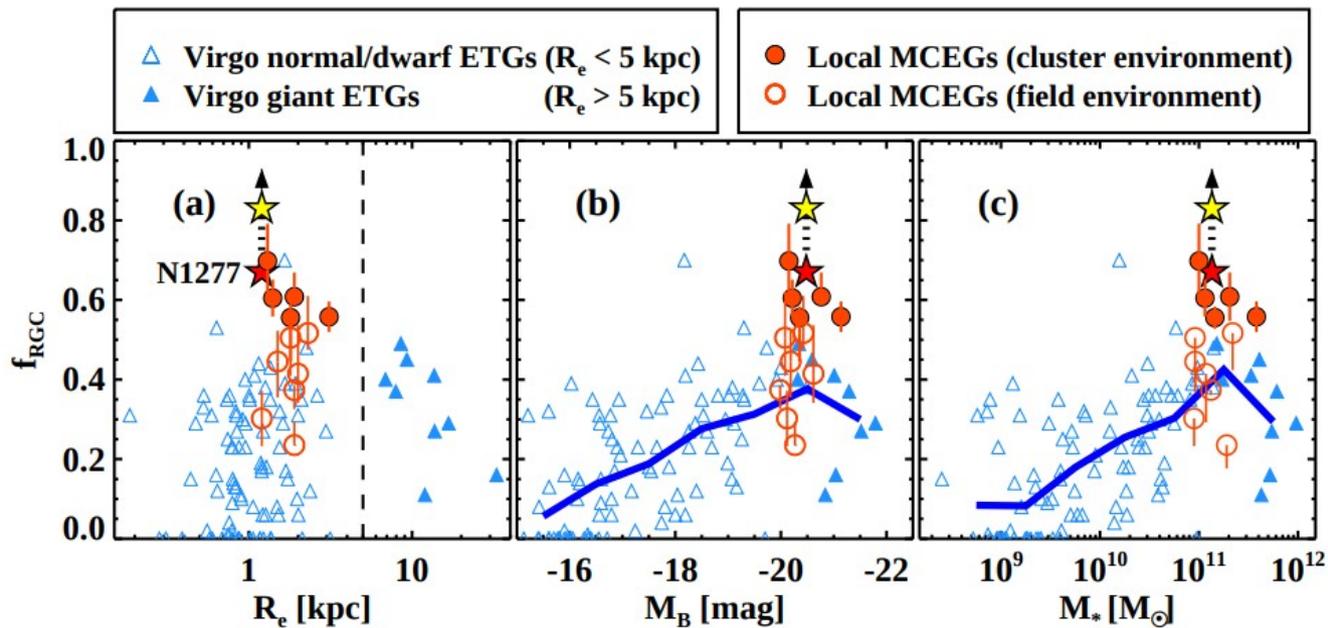


**Figure 17.** Red GC fractions ( $f_{RGC}$ ) vs. (a) effective radii ( $R_e$ ), (b) B-band absolute magnitudes ( $M_B$ ), and (c) stellar masses ( $M_*$ ) for the target MCEGs in this study in comparison with the Virgo ETGs (Côté et al. 2004; Peng et al. 2006, 2008, ACSVCS). Symbols are the same as Figure 16 but we mark the Virgo ETGs with  $R_e > 5$  kpc as filled symbols. Filled red circles mark the MCEGs in cluster environment and open red circles mark the MCEGs in field environment. The yellow star represents the value for NGC 1277 given in Beasley et al. (2018), and the red star denotes the value derived using the fixed color criterion as in this study. The blue solid lines in (b) and (c) represent the median of the red GC fractions for the Virgo ETGs along with the absolute magnitudes and stellar masses.

# results

- Проведен поиск шаровых скоплений в 12 близких MCEGs, для этого использована фотометрия в фильтрах HST/WFC3 F814W/F160W. Зависимость масса-радиус для этих MCEGs отличается от таковой для массивных локальных эллиптических галактик в скоплениях, но похожа на зависимость для red nuggets на  $z=2$ .
- CMDs показывают, что в большинстве MCEGs находится много шаровых скоплений. Возможность детектирования ШС с определенной звездной величиной зависит от расстояния до галактики (абсолютные  $M_I \approx -13.0$  to  $-8.5$  mag).
- Распределения по цвету для кандидатов в ШС со значением  $I_{814,0} < 25.0$  mag показывают, что MCEGs демонстрируют доминирующую широкую компоненту в диапазоне  $0.0 < (I_{814} - H_{160}) < 1.1$ , в основном это ШС изучаемых галактик
- Авторы оценивают долю ШС используя фиксированное разделение по цвету  $(I_{814} - H_{160})_0 = 0.49 \pm 0.04$ . Доля красных ШС в MCEGs примерно на 0.2 выше чем для гигантских эллиптических галактик в Деве с той же массой. Некоторые MCEGs должны показывать еще большие доли красных ШС, например как NGC 1277, известная реликтовая галактика
- Эти результаты предполагают, что большинство красных ШС были сформированы рано в массивных галактиках и что большинство MCEGs претерпели мало событий мерджинга с тех пор, как стали red nuggets 10 Млрд лет назад. Соответственно они являются реликтовыми галактиками